

# INDUSTRIAL ASSESSMENT OF OVERALL AIRCRAFT DRIVEN LOCAL ACTIVE FLOW CONTROL

**Matthias Lengers\***  
**\*Airbus Operations GmbH**

**Keywords:** *flow separation, high-lift, wing-pylon*

## Abstract

*A multidisciplinary study was conducted focusing on the implications of localized stall-delaying flow control on commercial aircraft configurations with the objective of enabling a closely-coupled engine integration without high-lift penalties. Preliminary design methods were used to quantify benefits and drawbacks of various disciplines supported by a wind tunnel test campaign.*

## 1 Introduction

Only a few published studies, such as [1] [2] [3] [4] [5], are focusing on the multi-disciplinary implications associated to the integration of stall-delaying flow control into state-of-the-art commercial aircraft.

The work presented here, is concentrating on a local wing leading edge application of active flow control, addressing disciplines in the frame of an overall aircraft design process as well as trying to assess the aerodynamic feasibility and potential of flow control.

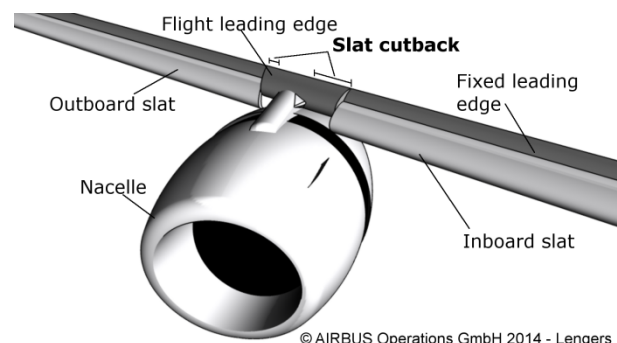
### 1.1 Historic flow control implementation

As argued by [6] flow control has been in the scope of research for a significant time frame and often time is dated back to the early work of Prandtl [7]. However, except for a few flight tests, such as [8] [9], active flow separation control has not found its way into the application on commercial air transport vehicles. In the middle of the last century this technology was introduced to military configurations of large variety. Whereas, the enhancement of the flap flow was dominating

the overall development, a few aircraft were also equipped with leading edge flow control devices, which will be in the focus of this work.

- Dassault Etendard IV Marine [10] [11]
- McDonnellDouglas F-4B Phantom2 [12]
- Blackburn Buccaneer [13]
- NA F100A Super Sabre [14]
- Boeing YC-14 [15] [16]
- C-8A QSRA NASA 715 [17]

In conclusion, the technology often-times provided great aerodynamic benefits, while the integration into the overall aircraft was proofed to be challenging. High angles of attack became possible revealing handling qualities limits [14], but also synergies between stall angle protection and wing anti ice were found [15] [16]. Engine bleed penalties during take-off [18] occurred and additional system and structural efforts due to the hot airflow were necessary. Additionally, backup measures had to be taken to tackle engine failures [15] [16] [17]. Extending the common lift envelope also lead to reduced stall indications [14] and revised trim settings [14]. Nevertheless, for some successful military fighters [12], such as the Phantom, flow control earned its way onto the aircraft.



© AIRBUS Operations GmbH 2014 - Lengers

Fig. 1. Schematic high lift device cutback

## 1.2 Flow control use case for commercial airframes

In contrast to high lift performance-driven military types, commercial aircraft are much more constrained by the safety, economics, passenger-comfort and ground infrastructure. Accordingly, a flow control integration-process cannot neglect those boundaries by dominating the overall aircraft configuration.

Therefore, this technology is rather anticipated as a local improvement and enabler of other technologies for the next aircraft.

Such an area prone for flow improvement is shown in Fig. 1. Contributed to the current trend of increasing by-pass ratios and associated nacelle diameters, future engines will most likely be coupled closer to the wing. This is due to the fact that an underwing mounting of the engines is limited by the ground-clearance and the close-coupling is preferred over a heavy landing gear length extension.

This in turn has implications on the deployment of the inboard leading edge high lift devices. Whereas the A300/A310 were equipped with continuous-slats, today's aircraft already incorporate a high-lift-device-cutout in order to accommodate for their deployment. When increasing the engine nacelle the high lift devices need to be cut-back even further in order to prevent clashes with the nacelle or the thrust reverser.

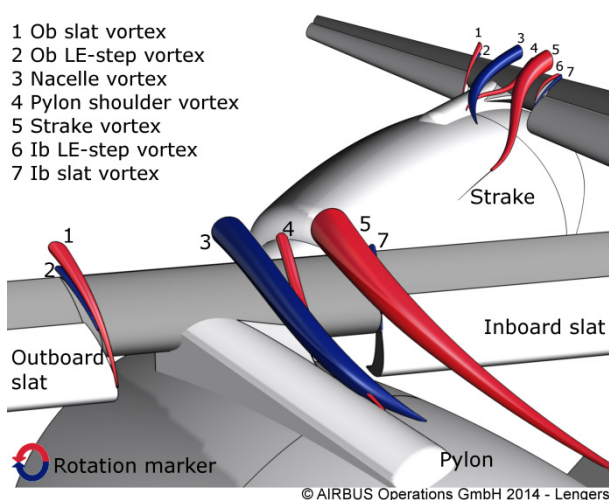


Fig. 2. Schematic representation of the vortices dominating the region at the pylon-wing junction (based on [19] [20])

## 1.3 Flow topology of the wing-pylon junction

The air flow in the vicinity of the inboard pylon-wing junction can be characterized by multiple vortex phenomena as shown in Fig 2. At high angles of attack the high vorticity interacts with the wing cross-flow and an additional upwash. This upwash is linked to the nacelle ring-wing effect [21] (Fig 3.) and the result is a complex three-dimensional flow field, about which only a few publications can be found [19] [22] [20] [21].

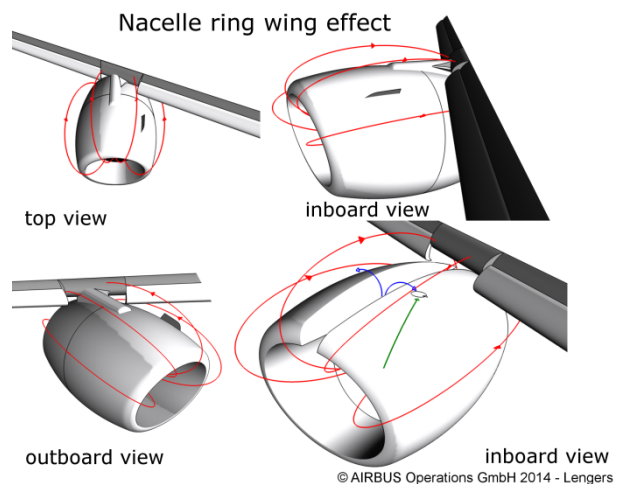


Fig. 3. Simplified schematic representation of nacelle ring-wing effect inspired by [21]

## 1.4 Multi-disciplinary aspects of local flow control at the high-lift-device-cutback

Depending on the span-wise wing location of the overall-stall onset, the high-lift device cutback amounts to significant losses in the maximum lift  $CL_{max}$  as quantified in [23] to be about  $\Delta CL_{max} \sim 0.1$ . For typical short-range aircraft with wing area sized by the maximum lift coefficient those levels require corrective actions. One example of such existing solution is the Sealing Krüger of the Boeing 777 and 787. Due to Nield [24] the cutback is not impacting the highest lift due to the existence of the strake/chine. The extra high-lift device between the pylon and slat serves the purpose of drag reduction [24]. Nevertheless, for configurations with strake performance already accounted for in the baseline configuration, a short-fall in  $CL_{max}$  as well as a positive drag increment are to be expected.

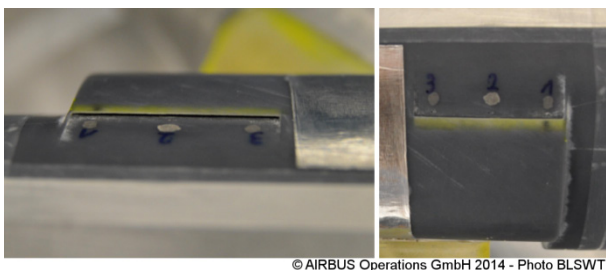
Pneumatic active flow control methods (e.g. [14] [25] [26] ) offer the opportunity to mitigate such losses by locally improving the flow. This lever a small improvement up to a significant overall wing stall-delay without imposing geometrical constraints, in comparison to a high lift device deployment.

## 2 Empirical and analytical assessments

The assessment of this new flow control application was conducted on analytical level in form of a preliminary design platform computation and additional Computational Fluid Dynamics (CFD) computations [27] [28]. An empirical foundation was given to the assumptions by an in-house wind tunnel test campaign as well as the validation and calibration of the aircraft design methods with existing aircraft values.

### 2.1 Wind tunnel assessment

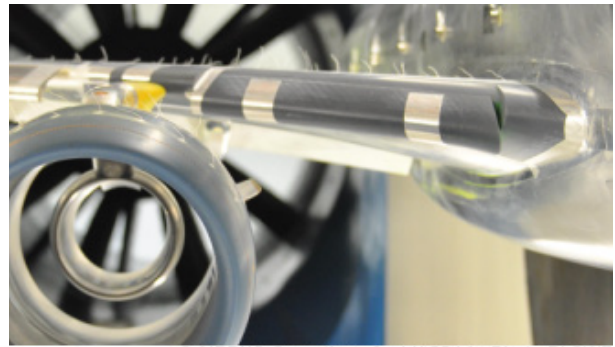
A representative industrial single-aisle half-model was tested in the Bremen Low Speed Wind Tunnel (BLSWT) facility yielding to a Reynoldsnumbers of  $1.6E06$  at a Mach-Number of 0.2. The model, which is shown in Fig. 5., was equipped with a Through-Flow Nacelle (TFN) as well as a conventional high lift system. The inboard leading edge high lift device was a drooped leading edge device with a 300 mm cutback in respective aircraft scale. This so called droop-nose-device (DND) was manufactured by means of rapid prototyping, which allowed to integrate a pressurized duct in the droop nose and yielded to a flow control exhaust piece as shown in Fig. 4 and 6.



© AIRBUS Operations GmbH 2014 - Photo BLSWT

Fig. 4. Upstream view and top view of slot geometry on the wing leading edge inboard of the engine-pylon

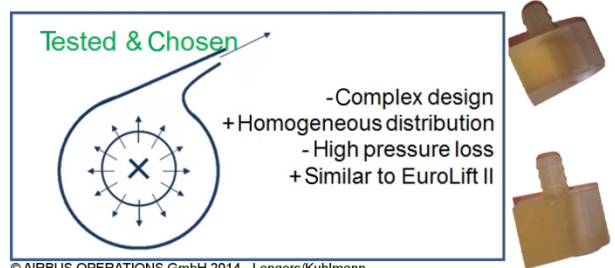
The steady-blowing flow control exhaust was designed to be exchangeable and represented a part of the flight leading edge in the span-wise range of the droop-nose cutback. As a result of pre-tests the plenum was pressurized via a piccolo tube, similar to the pressure distribution in a slat equipped with wing-anti-ice.



© AIRBUS Operations GmbH 2014 - Photo BLSWT

Fig. 5. Half-model in low-Reynoldsnumber test facility in Bremen

For the purpose of the jet-analysis the static pressures at the slot exit were measured as well as the pressure and the total temperature in the plenum. By using the isentropic flow relations, combined with Braggs [29] vena-contracta computations, the jet properties were assessed. In the course of the test, theoretical jet Mach-Numbers greater than one were calculated and most runs were conducted with an under-expanded jet [27] (as in [30]).



© AIRBUS OPERATIONS GmbH 2014 - Lengers/Kuhlmann

Fig. 6. Blowing device configuration

### 2.2 Multidisciplinary assessment

The empirical assessment by means of the wind tunnel test campaign targeted the physical feasibility, whereas the evaluation with an in-house Target Setting Platform (TSP) was undertaken to assess the benefit on overall aircraft level.

### 2.2.1 Overall aircraft design methods

As schematically depicted in Figure 7., an Overall Aircraft Design (OAD) study was constructed [31] [32] using the commercial Integration Platform Isight 5.6 by Dassault Systèmes Simulia Corp. [33] populated with Airbus preliminary design tools.

determined. Known legacy high speed polars were decomposed into their frictional and induced drag components and modified according to the geometrical difference between current design and reference. The low speed performance assessment was conducted with an Airbus semi-empirical design tool. This software optimized the clean wing twist-

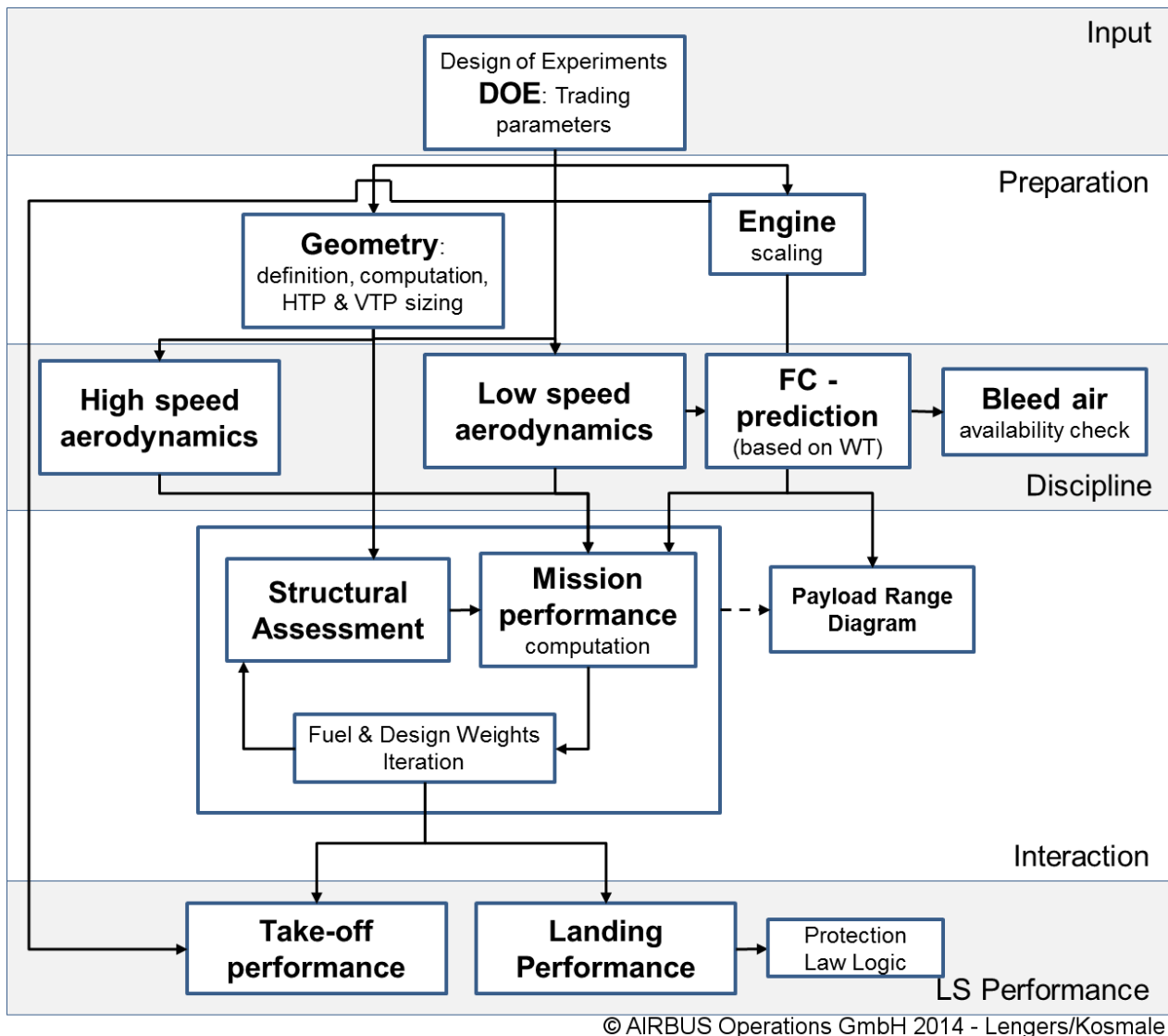


Fig. 7. Schematic overview of multidisciplinary evaluation

As an initial step, a Design of Experiments (DOE) method defined the basic trading parameters and the main aircraft data, such as wing- and flap- area as well as the flow control parameters. In a subsequent preparation-step, the engine was scaled up and the geometry was computed and visualized. With the geometry being available, the high speed performance was

distribution to a cruise design point and subsequently used a sectional panel method coupled to a lifting line method both being calibrated with wind tunnel and flight test data to determine the polar for each high lift configuration. The  $CL_{max}$  gain due to flow control as well as the cutback trade curve were based on legacy wind tunnel entries and

integrated into the software by means of increments. On the basis of measured data from the wind tunnel test, take-off drag increments were added to the low speed aerodynamic coefficients. Referencing to existing engine bleed air off-take- percentages, it was assessed if a limit was reached when including the required flow control mass flow.

Due to the additional flow control system weight and changes in the high lift system, a Mass-Performance-Loop was integrated to account for the resizing effects. This loop incorporated a calibrated method based on finite element methods with the capability to predict weights for the structural as well as the system items. With updated aircraft design weights, such as e.g. the Max Take-off Weight (MTOW) and Operating Weight Empty (OWE), the mission performance was computed. All mission phases were accounted for and the cruise was optimized via step-climb and by choice of the best cruise altitude. Since the required fuel weight had an impact on the structural wing sizing the mass-performance loop was iterated to yield to the convergence of the design weights.

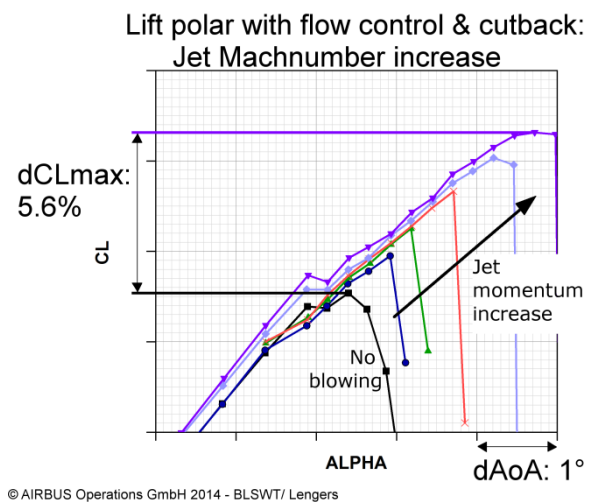
Following the determination of the weights and the aerodynamic low speed performance, the take-off- and the landing performance was computed yielding to the two key variables, that is the Take-Off Field Length (TOFL) and the approach speed ( $V_{app}$ ). While the approach speed is determined by a static equilibrium with consideration of different limitations, the Take-off performance was computed time dependently, also considering the engine failure. Based on the wind tunnel assessment the flow control performance was only considered for landing purposes, whereas the measured drag-increments due to the cutback were included in the low speed aerodynamics.

### 3 Results of wind tunnel test and multidisciplinary evaluation

The primary results of the wind tunnel campaign and the multi-disciplinary assessment are presented in the following.

#### 3.1 Wind tunnel test results

As shown in Figure 8. the leading edge flow control in the span-wise extend of the cutback yielded to an angle of attack protection similar to the effect of a slat. By increasing the jet Machnumber the flow stays attached up to higher degrees of attack leading to a gain of up to 5.6 percent  $CL_{max}$  and a stall incidence increase of 2.3 degrees.



© AIRBUS Operations GmbH 2014 - BLSWT/ Lengers

Fig. 8. High lift polar with flow control

In consideration of the span-wise extend of about 300 mm this indicates the very powerful leverage-effect of localized flow control.

Without the use of static pressure tabs in surface of the model the investigation focused on force measurements and oil-flow visualizations. On the basis of photographs, such as shown in Figure 9., schematic flow features (Figure 10. and 11.) were extrapolated from the vortex footprints manifested in surface streaks with low oil-color collection. In Figure 10. three main features are outlined. Firstly, the strake boundary separating the inboard- from the outboard-flow, secondly the strong cross flow trailing the droop-nose and thirdly the flow control jet merging into the strake boundary. As indicated in Figure 10. the angle between the cross-flow and the strake footprint yields to a flow-component-split in upstream and downstream direction. The upstream component was found to determine the inboard wing stall.

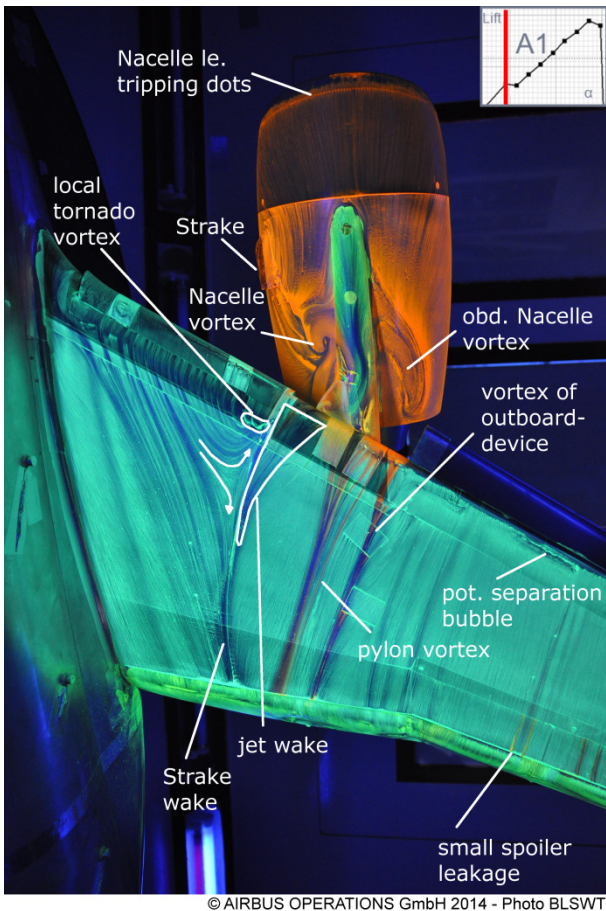


Fig. 9. Oilflow visualization with flow control – the jet wake outlined by a triangle

The oil-flow visualizations showed large oil-collections in this area, characterized by an anti-clockwise recirculation with a vertical axis. This characteristic recirculation was found to be much smaller and more stable with the flow control jet turned on.

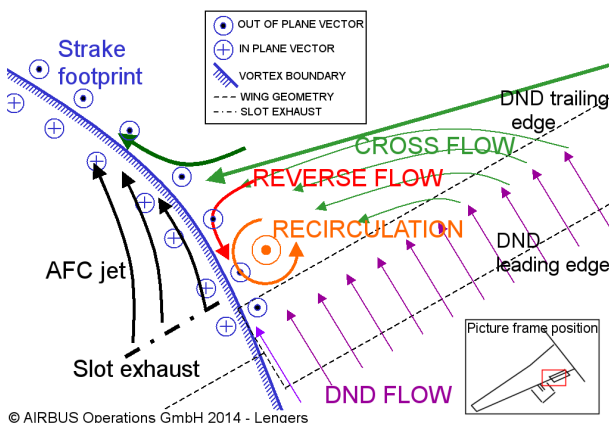


Fig. 10. Surface oilflow streamlines with flow control (angel  $A1$ )

The jet, on the outboard side of the strake footprint, merged triangularly into the strake vortex, which was found to be significantly strengthened.

Going to higher angles of attack, while using flow control, the strake vortex stayed bound to its position, passing the outboard end of the inboard droop nose as shown in Fig. 10 for lower angles.

Without flow control however, the strake vortex is shifted much further inboard as depicted in Figure 11. Due to the absence of the flow control jet, two recirculation-regions develop on the inboard wing.

Therefore, it was concluded that the jet had a stabilizing effect on the strake. However, while modifying the high lift configuration it was also found that the most powerful flow control case achieved almost the same lift gains as the strake, whereas the combination of both was almost cumulative.

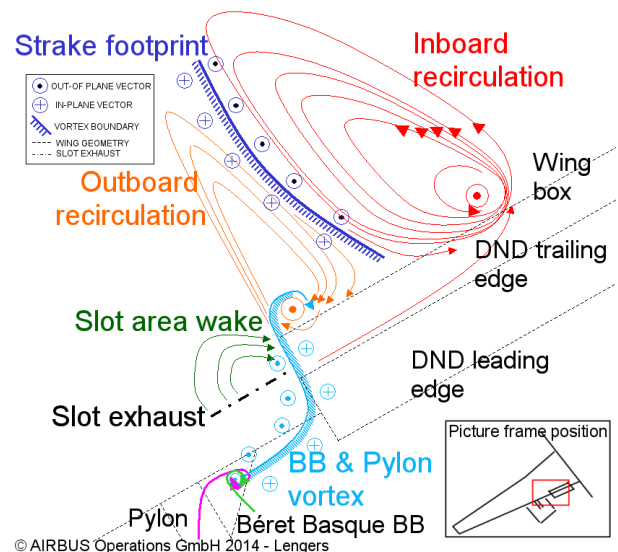


Fig. 11. Surface oilflow streamlines at stall without flow control (angel  $A1 + 0.75^\circ$ )

### 3.2 Results of the multidisciplinary assessment

#### 3.2.1 System

The flow control system, which was investigated, can be characterized by its high degree of commonality with the state of the art wing anti-ice system. Both of the latter are

supplied with High Pressure (HP) bleed air from the engine core cooled down to about 180°C by the engine pre-cooler. Both systems also exhaust this air through structures located in the leading, being the slat or in this case the clean leading edge. Additionally, due to the nature of the local AFC system and its operation during a short fraction of the flight, it is concluded that such a system will have to be linked to the pressure source of the Environmental Control System (ECS), which in this case is the bleed air infrastructure. On the basis of the latter, an internal system safety analysis was conducted, which identified the engine failure cases to be a significant driver. While already considering cross-bleed scenarios from one wing to the other, it can be concluded that an improvement of the flow control system safety beyond the failure probability of the engines is not possible and therefore a completely fail-safe system seems unrealistic.

The assembly room in the leading edge inboard of the pylon is densely packed and incorporates:

- Bleed air duct and leakage sensing wires
- Engine management cables
- Torque-shaft for the high lift device motorization
- Cables for electric power distribution.

Nevertheless, it has to be accounted for the fact that a cutback of the current high-lift device generates space. The cut-off part belonging to the high lift device, now becomes part of the flight leading edge. Therefore, the largest challenge was identified to be the integration of the flow control valve into this location.

Operability aspects were considered on a first level basis and especially the contamination of the flow control devices with e.g. rain, ice, sand and de-icing fluid was considered yielding to the necessity of a drainage capability.

### *3.2.2 Energy provision*

On the basis of a state of the art engine, a bleed air availability study was conducted. For the assessment three points in the timeline of a typical single aisle standard landing approach

were considered in order to account for the correct approach idle thrust coefficients, which is not only driven by the flight equilibrium, but also by the necessary take-off go-around performance provision. The outcome showed an increased thrust in the approach phase, which is significantly higher than the descent idle setting, which can also be negative.

The bleed air assessment was conducted with a fixed maximum relative off-take value rather than modeling the complex cycle process. Thus, it was only checked whether sufficient levels of bleed air are available. For this assessment three different cases were considered:

- Normal conditions (ECS on)
- Icing conditions (ECS & Wing Anti Ice (WAI) on)
- One Engine Inoperative (OEI)

However, due to two reasons a use of flow control during OEI seems questionable. Firstly the use of high pressurized air in the area of a shut-down engine is a potential fire hazard, secondly, an automatic opening of the cross-bleed valve is necessary in a matter seconds to avoid severe asymmetry flights.

### *3.2.3 Handling Qualities*

Due to the “slat effect” of the leading edge flow control system, that is the elongation of the lift polar, a failure only impacts high angles of attack. Associated to the lift loss such a potential inboard wing stall is linked to a beneficial pitch down motion and a small induced rolling moment.

A study was undertaken to assess the integration into the protection law logic. By assessing all limiting  $CL_{max}$  scenarios, including the failure of the wing anti-icing system, a natural limit of the lift enhancement was found. This limit assures that in the normal law a flow control failure is not accessing the flow critical incidence range.

### *3.2.4 Noise impact*

The wind tunnel campaign included a rudimentary assessment of the noise impact onto imaginary cabin window positions on the

fuselage. Small microphones were attached to the fuselage of the wind tunnel model. The preliminary assessment of the sound-pressure-level, weighted with an A-filter, showed no significant difference due to the jet operation.

### 3.2.5 Structural integration

The weight of the flow control system was assessed based on empirical bleed air system weight data [32] and integrated into the preliminary aircraft design process. By relying on CFD assessments [27] [28] it was also possible to get a first order of view on the heat footprint of the configuration as tested in the wind tunnel campaign. It can be seen in Fig. 12. that the heat wake narrows down for higher angles of attack. Nevertheless, considering bleed air failure cases the temperatures close to the slot exceed the maximum CFRP temperatures of about 80 °C. Consequently, a metallic wing would be more suitable for such a concept.

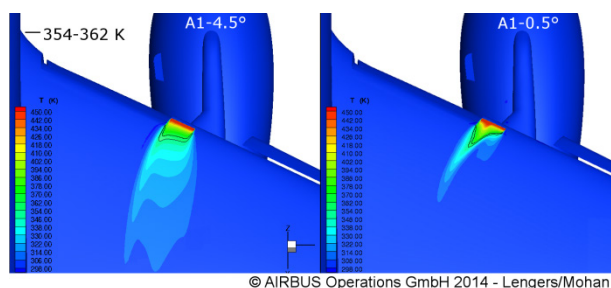


Fig. 12. Jet heat wake derived from CFD computations with the DLR-TAU code (based on computation from [28])

### 3.2.6 Transonic aerodynamics

By using an assessment method, provided by parasitic drag specialists it was found that the slot width and exhaust-surface-angle were the strongest driver for the slot cruise drag increment, which however was negligible for the current application. Nevertheless, it was integrated into the OAD assessment.

Additionally, with respect to the OAD wing area trade the constant sweep and little changes in the aspect ratio justified to ignore any buffeting effects.

### 3.2.7 Overall aircraft design

In order to make a fair assessment for a new aircraft-design three scenarios were considered:

- Reference single aisle aircraft
- Reference aircraft with cutback
- Reference aircraft with cutback and stall improvement based on medium wind tunnel jet momentum value, that is  $C_{\mu} = 0.1798$  percent

The introduction of a moderate cutback reduced the  $CL_{max}$  of the configuration FULL by about 3.5 lift counts and required a mitigation in order to maintain the desired approach speed.

For each configuration an optimum was chosen based on a variation of the flap- and wing-area. This optimum targeted the minimum block-fuel consumption for the design mission by respecting the most critical constraints:

- Take-off field length of a critical airport
- Maximum approach speed
- Wing fuel capacity of the largest family member for the longest mission

In Fig. 13 the Block-Fuel surface plot for the flow control case is shown. The left hand axis shows the flap area increase, the right hand axis represents the wing area increase. It can be seen that the optimal combination of wing area, flap area and fuel capacity is limiting for the flow control case.

The locations of the respective optima are indicated by dots and projected onto the AFC-Block-Fuel surface-plot.

In order to recover  $CL_{max}$ , lost due to the cutback, three options are available assuming there is no further conventional leading edge high lift potential:

- Flap area increase
- Wing area increase
- Active flow control

The increase of the flap area at unchanged high lift deflection angles yielded to a higher take-off drag, reduced the fuel capacity and increased the secondary wing weight structure. Consequently, the TOFL at high altitude and high temperatures became constraining for the scenarios with leading edge cutback, whereas the reference optimum was defined by the fuel margin and the approach speed.

Maintaining the approach speed by increasing the wing area reduced the Lift over Drag Ratio (LoD) due to higher surface friction drag and resulted in increased fuel consumption at unchanged flight altitudes. As an additional effect of secondary importance the empennage area also increased due to its link to the wing area.

Conducting this assessment for every configuration, the high-lift device cutback configuration showed 0.5 percent higher fuel consumption than the reference.

The flow control implementation was however able to reduce this penalty to 0.13 percent including a bleed air system weight increase of 21.4 kg.

The bleed air consumption was considered and amounted to 42.75 percent of the maximum possible bleed air quantity, including ECS and WAI. Considerations to use a failed engine to provide bleed air to both wings (outlined as problematic above) amounted to about 92.5 percent of the available mass flow. This was due to the high ECS setting, which however according to discussions with specialists could be turned off shortly in the phases of demand, as it is sometimes done during take-off.

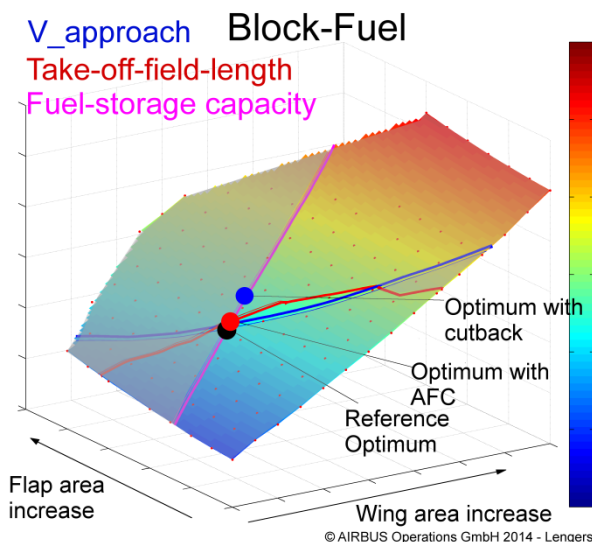


Fig. 13. Block fuel surface plot with flow control- constraint by the colored lines

Besides the flow control-related efficiency improvement, the engine-integration-enabler-effect was not quantified within this study. However, the idea remains to use the flow

control technology to integrate very high bypass ratio engines to future wings. If the fuel consumption reduction, due to this new engine, is additionally considered the benefit is much larger.

Furthermore, improvements in the system safety could be used to increase the maximum lift performance to levels beyond the current legacy performance. This could reduce the block-fuel even further and generate additional benefits.

#### 4 Conclusions

A method of local stall-delaying flow control, mitigating the maximum lift penalty of closely coupled engines, was presented and assessed. The feasibility was proven by a low-Reynoldsnumber wind tunnel test and found to create synergetic effects with the Strake vortex. The local device also showed synergies with the current wing anti-ice system and could therefore be integrated without large and unconventional configuration-changes. The safety assessment pointed to the non-failsafe character of the implementation, which however is not impacting the flight in normal law. The overall aircraft design concluded that the cutback penalty can be eliminated and further potential besides the engine integration seems realistic. A flight test could be undertaken with relatively low effort in comparison to the flight test effort of large flow control systems. This could not only validate the technology but also enable to get valuable insights about the use of flow control for future aircraft.

#### 5 Acknowledgements

The author dearly thanks his colleagues in the Flight Physics Domain, the Future Projects Office and R&T Domain of Airbus for the support, collaboration and many fruitful discussions. Especially, Daniel Reckzeh, Ulrich Scholz, Prof. Dr.-Ing. W. Nitsche, Hendrik Friedel, Dr. Heribert Bieler, Adrian Eberle, Dr. Martin Dreyer, Eldert Akkermann. The author is also very grateful for the thesis work involved,

conducted by Andrea Resmini, Maximilian Kosmale, Jithin Mohan and Lutz Bittner.

## References

- [1] J. D. McLean, J. D. Crouch, R. C. Stoner, S. Sakurai, G. E. Seidel, W. M. Feifel and H. M. Rush, *Study of the application of separation control by unsteady excitation to civil transport aircraft*, NASA CONTRACTOR REPORT NASA CR-1999-209338, Prepared by the Boeing Commercial Airplane Group for National Aeronautics and Space Administration Langley Research Center, Seattle, 1999.
- [2] W. J. Crowther, Separation control on a trailing-edge flap using air jet vortex generators, *JOURNAL OF AIRCRAFT*, vol. 43, pp. 1589-1593, September-October 2006.
- [3] S. C. Liddle and W. J. Crowther, *Systems and certification issues for active flow control systems for separation control on civil transport aircraft*, in 46th AIAA Aerospace Sciences Meeting and Exhibit, 7 - 10 January, Reno, Nevada, 2008.
- [4] M. Jabbal, S. C. Liddle and W. J. Crowther, Active flow control systems architectures for civil aircraft, *JOURNAL OF AIRCRAFT*, vol. 47, pp. 1966-1981, November-December 2010.
- [5] C. Werner-Spatz, *Flugzeugesamtentwurf mit Zirkulationskontrolle am Hochauftriebssystem*, vol. 1, Braunschweig: Technische Universität Braunschweig - Institut für Flugzeugbau und Leichtbau: Shaker, 2010.
- [6] W. J. Crowther, M. Jabbal and S. C. Liddle, "Flow control fallacies: a review of common pitfalls in flow control research," *Proceedings of the Institution of Mechanical Engineers Part G: Journal of Aerospace Engineering*, no. 255, pp. 1-11, 2011.
- [7] M. Zdravkovich, *Flow Around Circular Cylinders: Volume 2: Applications*, vol. 2, Oxford: Oxford Science Publications, 2003, pp. 944-945.
- [8] J. C. R. Taylor, *Flight test result of a trailing edge flap designed for direct-lift control*, NASA CONTRACTOR REPORT NASA CR-1426, Prepared by THE BOEING COMPANY for NATIONAL AERONAUTICS AND SPACE ADMINISTRATION Ames Research Center, Seattle, 1969.
- [9] L. B. Gratzler and T. J. O'Donnell, Development of a blc high-system for highspeed airplanes, *JOURNAL OF AIRCRAFT*, vol. 2, pp. 477-484, 1965.
- [10] P. Trichet, *Paperclip, french style*, in 47th AIAA Aerospace Sciences Including The New Horizons Forum and Aerospace Exposition, Orlando, 2009.
- [11] G. V. Lachmann, *BOUNDARY LAYER AND FLOW CONTROL - ITS PRINCIPLES*, vol. 1, Oxford: Pergamon Press, April 1961, p. 591.
- [12] L. K. Loftin, *Quest for Performance - The Evolution of Modern Aircraft*, Washington, DC: NASA-Scientific and Technical Information Branch, 1985.
- [13] S. F. J. Butler, *Low-speed wind-tunnel tests on a sweptback wing model (buccaneermark i) with blowing at the wing leading edge and blowing over the and drooped ailerons*, Ministry of Aviation Supply, Aeronautical Research Council, Reports and Memoranda, Aerodynamics dept., Farnborough, 1971.
- [14] C. Q. H, S. B. Anderson and R. C. Innis, *Flight investigation of the low-speed characteristics of a 45° swept-wing boundary-layer control applied to the leading- and trailing-edge flaps*, NATIONAL AERONAUTICS AND SPACE ADMINISTRATION Ames Research Center, Moffet Field, 1960.
- [15] T. C. Nark, Design, development and flight evaluation of the boeing yc-14 usb powered-lift aircraft, in *AGARD CONFERENCE PROCEEDINGS 71st Meeting; Symposium, High-lift system*, 1993.
- [16] H. L. Ernst and A. Gupta, YC-14 system for leading-edge boundary-layer control, *JOURNAL OF AIRCRAFT*, vol. 13, pp. 149-152, February 1976.
- [17] M. D. Shovlin and J. A. Cochrane, *An overview of the quiet short-haul research aircraft program*, National Aeronautics and Space Administration, Ames Research Center, Moffet Field, 1978.
- [18] W. Kelly, S. B. Anderson and R. C. Innis, *BLOWING-TYPE BOUNDARY-LAYER CONTROL AS APPLIED TO THE TRAILING-EDGE FLAPS OF A 35° SWEPT-WING AIRPLANE*, NATIONAL ADVISORY COMMITTEE FOR AERONAUTICS, Moffet Field, California, 1985.
- [19] A. Haines and A. Young, *Agardograph 323 - scale effects on aircraft and weapon*, AGARD, 1994.
- [20] R. Emunds, Leading edge vortex system of the A380 at high angles of attack in, in *Third Symposium "Simulation of Wing and Nacelle Stall*, Braunschweig, 2012.
- [21] D. Schwetzler, *A330 Analysis of flow interaction between through-flow nacelle and wing in landing configuration*, Deutsche Airbus Internal Technical Report, Bremen, 1991.
- [22] H. Freiherr von Geyr, N. Schade, J. van de Borg, P. Eliasson and S. Esquieu, *Cfd prediction of maximum lift effects on realistic high-lift-commercial-aircraft-configurations within the european project Eurolift II*, in 25th AIAA Applied Aerodynamics, Miami, 2007.
- [23] P. May, *Aircraft Airfoil with close-mounted engine and leading edge high lift system*. Germany/Bremen Patent 6,364,254, 2 April 2002.

- [24] B. N. Nield, An overview of the boeing 777 high lift aerodynamic design, *Aeronautical Journal*, 1995.
- [25] M. Bauer, J. Lohse and W. Nitsche, *Experimental investigation of the high-lift performance of a two-element configuration with a two-stage actuator system*, *JOURNAL OF AIRCRAFT*, 2014.
- [26] P. Scholz, M. Casper, J. Ortmann and C. J. Kähler, Leading-edge separation control by means of pulsed vortex generator jets, *JOURNAL OF AIRCRAFT*, vol. 46, pp. 837-846, 2008.
- [27] A. Resmini, *Study of Active Flow Control at the Pylon-Wing Intersection by Means of 3D CFD*, Master Thesis report at Airbus Operations GmbH supervised by U. Scholz and M. Lengers, Bremen, 2012.
- [28] J. Mohan, *Application of local flow control in transport aircraft using numerical simulation*, Master Thesis report at Airbus Operations GmbH supervised by M. Lengers and U. Scholz, Bremen, 2013.
- [29] S. L. Bragg, Effect of compressibility on the discharge coefficient of orifices and convergent nozzles, *JOURNAL MECHANICAL ENGINEERING SCIENCE*, vol. 2, no. 1, pp. 35-44, 1960.
- [30] R. J. Englar, *EXPERIMENTAL INVESTIGATION OF THE HIGH VELOCITY COANDA WALL JET APPLIED TO BLUFF TRAILING EDGE CIRCULATION CONTROL AIRFOILS*, DAVID W. TAYLOR NAVAL SHIP RESEARCH AND DEVELOPMENT CENTER, Bethesda, 1975.
- [31] M. Kosmale, *Methodological Design and Development of a Multidisciplinary Aircraft Study with a Primary Focus on the Assessment of High Lift Configurations*, Master Thesis report at Airbus Operations GmbH supervised by M. Lengers, Bremen, 2013.
- [32] L. Bittner, *IMPROVEMENT AND DEVELOPMENT OF A MULTIDISCIPLINARY OVERALL AIRCRAFT DESIGN STUDY WITH A FOCUS ON LOW SPEED FLIGHT SCENARIOS*, Master Thesis report at Airbus Operations GmbH supervised by M. Lengers, Bremen, 2013.
- [33] R. M. Finke, S. Schaufele, B. Wonneberger, C. Blondel, C. Lynas, H. Leach and M. Duffau, Benefits of Integration Platforms in Preliminary Aircraft Design, in *SIMULIA Customer Conference*, Barcelona, 2011.

## **6 Contact Author Email Address**

<mailto:Matthias.Lengers@airbus.com>

## **Copyright Statement**

The authors confirm that they, and/or their company or organization, hold copyright on all of the original material included in this paper. The authors also confirm that they have obtained permission, from the copyright holder of any third party material included in this paper, to publish it as part of their paper. The authors confirm that they give permission, or have obtained permission from the copyright holder of this paper, for the publication and distribution of this paper as part of the ICAS 2014 proceedings or as individual off-prints from the proceedings.